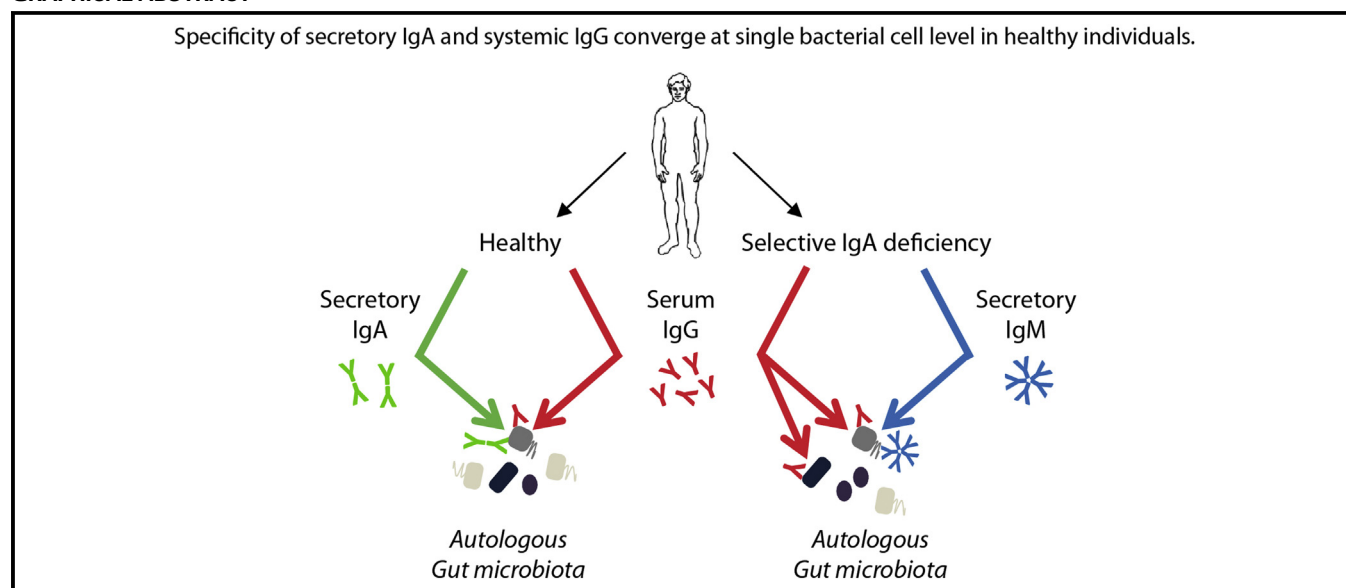


# Synergistic convergence of microbiota-specific systemic IgG and secretory IgA

Jehane Fadlallah, MD, PhD,<sup>a,\*</sup> Delphine Sterlin, PharmD, PhD,<sup>a,\*</sup> Claire Fieschi, MD, PhD,<sup>c</sup> Christophe Parizot, MSc,<sup>a</sup> Karim Dorgham, PhD,<sup>a</sup> Hela El Kafsi, PhD,<sup>a</sup> Gaëlle Autaa, MSc,<sup>a</sup> Pascale Ghillani-Dalbin, PharmD, PhD,<sup>a</sup> Catherine Juste, PhD,<sup>b</sup> Patricia Lepage, PhD,<sup>b</sup> Marion Malphettes, MD, MSc,<sup>c</sup> Lionel Galicier, MD, PhD,<sup>c</sup> David Boutboul, MD, PhD,<sup>c</sup> Karine Clément, MD, PhD,<sup>d,e</sup> Sébastien André, PhD,<sup>d</sup> Florian Marquet, PhD,<sup>d</sup> Christophe Tresallet, MD, PhD,<sup>f</sup> Alexis Mathian, MD, PhD,<sup>a</sup> Makoto Miyara, MD, PhD,<sup>a</sup> Eric Oksenhendler, MD,<sup>c</sup> Zahir Amoura, MD, MSc,<sup>a</sup> Hans Yssel, PhD,<sup>a</sup> Martin Larsen, PhD,<sup>a</sup> and Guy Gorochov, MD, PhD<sup>a</sup> *Paris, France*

## GRAPHICAL ABSTRACT



From <sup>a</sup>Sorbonne Université, INSERM, Centre d'Immunologie et des Maladies Infectieuses (CIMI-Paris), Assistance Publique-Hôpitaux de Paris (AP-HP), Groupement Hospitalier Pitié-Salpêtrière, Département d'Immunologie, Paris; <sup>b</sup>Micalis Institute, INRA, AgroParisTech, Université Paris-Saclay, 78350 Jouy-en-Josas, Paris; <sup>c</sup>Université Paris Diderot Paris 7, Department of Clinical Immunology, Hôpital Saint-Louis, Assistance Publique Hôpitaux de Paris (APHP), Paris; <sup>d</sup>Sorbonne Université, INSERM, UMRS1166, NutriOmics team, ICAN, Paris; and <sup>e</sup>Assistance Publique Hôpitaux de Paris, Nutrition department, Pitié-Salpêtrière Hospital, Paris; and <sup>f</sup>the Department of Surgery, Assistance Publique Hôpitaux de Paris, Pitié-Salpêtrière Hospital, Paris.

\*These authors contributed equally to this work.

The study was supported by Institut National de la Santé et de la Recherche Médicale (INSERM), Agence Nationale de la Recherche (MetAntibody, ANR-14-CE14-0013), and Fondation pour l'Aide à la Recherche sur la Sclérose en Plaques (ARSEP).

Disclosure of potential conflict of interest: The authors declare that they have no relevant conflicts of interest.

Received for publication February 20, 2018; revised August 24, 2018; accepted for publication September 4, 2018.

Corresponding author: Martin Larsen, PhD, or Guy Gorochov, MD, PhD, Centre d'Immunologie et des Maladies Infectieuses (CIMI Paris), Inserm UMR-S1135, 83 Boulevard de l'Hôpital, 75013 Paris, France. E-mail: [Martin.Larsen@sorbonne-universite.fr](mailto:Martin.Larsen@sorbonne-universite.fr). Or: [Guy.Gorochov@sorbonne-universite.fr](mailto:Guy.Gorochov@sorbonne-universite.fr).

0091-6749/\$36.00

© 2018 American Academy of Allergy, Asthma & Immunology

<https://doi.org/10.1016/j.jaci.2018.09.036>

**Background:** Commensals induce local IgA responses essential to the induction of tolerance to gut microbiota, but it remains unclear whether antimicrobiota responses remain confined to the gut.

**Objective:** The aim of this study was to investigate systemic and intestinal responses against the whole microbiota under homeostatic conditions and in the absence of IgA.

**Methods:** We analyzed blood and feces from healthy donors, patients with selective IgA deficiency (SIgAd), and patients with common variable immunodeficiency (CVID). Immunoglobulin-coated bacterial repertoires were analyzed by using combined bacterial fluorescence-activated cell sorting and 16S rRNA sequencing. Bacterial lysates were probed by using Western blot analysis with healthy donor sera.

**Results:** Although absent from the healthy gut, serum antimicrobiota IgG are present in healthy subjects and increased in patients with SIgAd. IgG converges with nonoverlapping secretory IgA specificities to target the same bacteria. Each individual subject targets a diverse microbiota repertoire with a proportion that correlates inversely with systemic inflammation. Finally, intravenous immunoglobulin

preparations target CVID gut microbiota much less efficiently than healthy microbiota.

**Conclusion: Secretory IgA and systemic IgG converge to target gut microbiota at the cellular level. SIgAd-associated inflammation is inversely correlated with systemic anticommensal IgG responses, which might serve as a second line of defense. We speculate that patients with SIgAd could benefit from oral IgA supplementation. Our data also suggest that intravenous immunoglobulin preparations can be supplemented with IgG from IgA-deficient patient pools to offer better protection against gut bacterial translocations in patients with CVID. (J Allergy Clin Immunol 2018;■■■:■■■-■■■.)**

**Key words:** Gut microbiota, anticommensal IgG, secretory IgA, IgA deficiency, common variable immunodeficiency, intravenous immunoglobulin

Gut commensal bacteria contribute to several beneficial properties to the host. This complex community provides metabolic functions, prevents pathogen colonization, and enhances immune development. A symbiotic relationship is maintained by using host innate and adaptive immune responses, such as antimicrobial compounds and mucus secretion, as well as IgA production.<sup>1,2</sup> However, the gastrointestinal tract remains an important reservoir for potential bloodstream infections that involve Enterobacteriaceae, *Enterococcus* species, or other gram-negative bacilli.<sup>3,4</sup> The physical gut barrier but also innate and adaptive immune mechanisms control host-microbiota mutualism, reducing the risk of bacterial translocation and systemic immune activation. Murine models of innate immune deficiency indeed have high serum IgG levels against gut microbiota.<sup>2</sup> Significant titers of IgG targeting *Escherichia coli* were also reported either in patients with inflammatory bowel diseases or in mice lacking secretory IgA.<sup>5,6</sup> Nevertheless, based on recent murine studies, the notion has emerged that induction of systemic IgG responses against gut symbiotic bacteria is not necessarily a consequence of mucosal immune dysfunction or epithelial barrier leakiness. Healthy mice actively generate systemic IgG against a wide range of commensal bacteria under homeostatic conditions, which are passively transferred to the neonates through the maternal milk.<sup>7</sup> Serum IgG that specifically recognizes symbiotic gram-negative bacteria confer protection against systemic infections by these same bacteria. Because such IgG target a conserved antigen in commensals and pathogens, they also enhance elimination of pathogens, such as *Salmonella* species.<sup>8</sup>

IgG-expressing B cells are present in human gut lamina propria during steady-state conditions and represent 3-4% of total gut B cells. About two thirds of IgG<sup>+</sup> lamina propria antibodies react with common intestinal microbes.<sup>9</sup> Inflammatory bowel disease is associated with a marked increase in numbers of gut IgG<sup>+</sup> B cells that might contribute to the observed increased serum anti-*E coli* IgG levels in these patients.<sup>9</sup> However, the extent to which gut IgG<sup>+</sup> B cells contribute to the serum IgG repertoire remains elusive. Focusing on anti-transglutaminase 2 antibodies, a low degree of clonal relationship between serum and intestinal IgG has been shown.<sup>10</sup> Altogether, it remains unknown whether secretory and serum antibacterial antibodies have identical targets or whether digestive and systemic antibody repertoires are shaped by distinct microbial consortia.

#### Abbreviations used

APC:	Allophycocyanin
CVID:	Common variable immunodeficiency
IVIG:	Intravenous immunoglobulin
OTU:	Operational taxonomic unit
PD-1:	Programmed cell death protein 1
PE:	Phycocerythrin
QIIME:	Quantitative Insights Into Microbial Ecology
sCD14:	Soluble CD14
SIgAd:	Selective IgA deficiency

In this study we report that human serum IgG binds a broad range of commensal bacteria. For the first time, we also demonstrate the convergence of intestinal IgA and serum IgG responses toward the same microbial targets under homeostatic conditions. Private antimicrobiota IgG specificities are induced in IgA-deficient patients but are not found in IgG pools from healthy donors, partially explaining why substitutive IgG cannot regulate antibody deficiency-associated gut dysbiosis and intestinal translocation. Finally, in both control subjects and IgA-deficient patients, systemic antimicrobiota IgG responses correlate with reduced inflammation, suggesting that systemic IgG responses contribute to gut microbiota confinement.

## METHODS

### Human samples

Fresh stool and blood samples were simultaneously collected from 30 healthy donors, 15 patients with selective IgA deficiency (SIgAd), and 10 patients with common variable immunodeficiency (CVID). Healthy donors were recruited from laboratory staff and relatives. Patients followed for clinical manifestations associated with antibody deficiencies were recruited from 2 French clinical immunology referral centers (the Department of Clinical Immunology at Saint Louis Hospital and the Department of Internal Medicine at Pitié-Salpêtrière Hospital, Paris, France).

The patient's inclusion criteria were as follows: (1) undetectable serum IgA levels (<0.07 mg/mL) in at least 3 previous samples in the past year or (2) either SIgAd (n = 15 patients with SIgAd) or association with IgG and/or IgM deficiency integrating a global antibody production defect (10 patients with CVID). Clinical and biological data were collected at inclusion. Surgical samples from histologically normal intestines were obtained from 12 donors undergoing gastric bypass or tumorectomy at Pitié-Salpêtrière Hospital, Paris, France.

Oral and written consent were obtained from patients and healthy donors before inclusion in the study.

### PBMCs and plasma

Thirty milliliters of blood were collected in ACD tubes (BD Vacutainer; BD, Franklin Lakes, NJ), and PBMCs were isolated by means of a density gradient procedure (Ficoll 400; Eurobio, Les Ulis, France) and then stored in liquid nitrogen after soft freezing in isopropanol. Supernatants were collected as plasma and immediately stored at -80°C.

### Stool collection and whole microbiota purification

Stool was collected immediately after emission in a container allowing anaerobic bacteria preservation (Anaerocult band; Merck, Darmstadt, Germany), placed in aliquots in a CO<sub>2</sub>-rich O<sub>2</sub>-low atmosphere, and stored at -80°C. Fecal microbiota were extracted by means of gradient purification under anaerobic conditions (Freter chamber), as previously described.<sup>11</sup> Briefly,

thawed feces were diluted in 1× PBS (Eurobio), 0.03% wt/vol sodium deoxycholate, and 60% wt/vol Nycodenz (Sigma-Aldrich, St Louis, Mo) and loaded on a continuous density gradient obtained by using a freeze-thaw cycle of Nycodenz solution. Fecal bacteria were obtained after ultracentrifugation (14,567g for 45 minutes at +4°C; Beckman Coulter ultracentrifuge, swinging rotor SW28; Beckman Coulter, Fullerton, Calif) and washed 3 times in 1× PBS (Eurobio) and 0.03% wt/vol sodium deoxycholate. The final pellet was diluted in 1× PBS–10% glycerol, immediately frozen in liquid nitrogen, and then stored at –80°C.

### Bacterial flow cytometry

Specific serum antibody levels against purified microbiota or cultivable strains were assessed by using a flow cytometry assay, as previously described.<sup>12</sup> Briefly, 10<sup>7</sup> bacteria (purified microbiota or cultivable strains) were fixed in a solution of 4% paraformaldehyde and simultaneously stained with a cell proliferation dye (eFluor 450; eBioscience, San Diego, Calif). After washing with 1 mL of a 1× PBS solution, cells were resuspended to a final concentration of 4 × 10<sup>8</sup> bacteria/mL in 1× PBS, 2% wt/vol BSA, and 0.02% wt/vol sodium azide solution. Then 10<sup>7</sup> bacteria were incubated in a 96-well V-bottom plate with a 10 µg/mL IgG solution (from either human serum or pooled human IgG Hizentra [CSL Behring, Paris, France] or human anti-TNF Remicade [MSD, Paris, France]) per condition. Immune complexes were washed twice with a 1× PBS, 2% wt/vol BSA, and 0.02% wt/vol sodium azide (200 µL/well at 4000g for 10 minutes at +4°C) and then incubated with secondary conjugated antibodies, either an isotype control mix or goat anti-human IgA–fluorescein isothiocyanate and goat anti-human IgG–A647 (Jackson ImmunoResearch Laboratories, West Grove, Pa). Acquisition of cell events was performed on a FACSCanto II flow cytometer (Becton Dickinson) after washing, and analysis was performed with FlowJo software (TreeStar, Ashland, Ore). Medians of fluorescence were used to measure serum IgG response levels against the cultivable strains. Intestinal IgA binding was quantified by using the same assay without incubation with serum immunoglobulins. Results are expressed as medians and minimum and maximum percentages throughout the article.

### Cytokine quantification

IL-6 and IL-10 levels were measured in plasma by using a 3-step digital assay relying on a Single Molecule Array (Simoa) technology HD-1 Analyzer (Quanterix, Lexington, Mass). Working dilutions were 1:4 for all sera in working volumes of 25 µL. Lower limits of quantification for IL-6 and IL-10 are 0.01 and 0.021 pg/mL, respectively.

### Soluble CD14 quantification

Soluble CD14 (sCD14) was quantified in plasma (400-fold dilution) by means of ELISA (Quantikine ELISA Kit; R&D Systems, Minneapolis, Minn). Experimental procedures followed the manufacturer's recommendations. The lower limit of quantification for sCD14 is 6 pg/mL.

### PBMC phenotyping

T-cell phenotyping was performed by using a combination of the following antibodies: CD3–H500, CCR7–phycoerythrin (PE)–Cy7, CD4–allophycocyanin (APC)–Cy7 (BD Biosciences), CD45RA–peridinin-chlorophyll-protein complex–Cy5.5 (eBioscience), CD8–A405 (Invitrogen, Carlsbad, Calif), and CD279–APC (BioLegend, San Diego, Calif). Acquisition of cell events was performed with a FACSCanto II flow cytometer (Becton Dickinson), and analysis was performed with FlowJo software (TreeStar).

### Intestinal B-cell phenotyping

Lamina propria was digested with collagenase A (Roche, Mannheim, Germany) in RPMI (Life Technologies, Grand Island, NY) for 30 minutes at 37°C. Lymphocytes were purified by means of centrifugation over a Ficoll 400 (Eurobio) and stained with the following antibodies: anti-CD45–APC–H7,

anti-CD19–BV421, anti-IgD–fluorescein isothiocyanate, and anti-CD27–PE–Cy7 (all purchased from BD Biosciences); anti-IgA–PE (Jackson ImmunoResearch, West Grove, Pa); or anti-IgG<sub>1</sub>–PE, anti-IgG<sub>2</sub>–AF488, and anti-IgG<sub>3</sub>–A647 (SouthernBiotech, Birmingham, Ala). Dead cells were excluded with the LIVE/DEAD Fixable Aqua Dead Cell Stain Kit (Invitrogen). Acquisition of cell events was performed with a FACSCanto II flow cytometer (Becton Dickinson), and analysis was performed with FlowJo software (TreeStar).

### Analysis of IgG-coated bacteria

Purified microbiota (10<sup>9</sup> per condition) was washed in 1× PBS and stained with isotype control (A647-conjugated goat IgG; Jackson ImmunoResearch) as a negative control or anti-human IgG–A647 (Jackson ImmunoResearch). Acquisition and sorting were performed on a 2-laser 2-way fluorescence-activated cell sorter (S3 cell sorter; Bio-Rad Laboratories, Hercules, Calif). Bacteria (10<sup>6</sup> per fraction) were collected and immediately stored at –80°C as dry pellets. The purity for both fractions was systematically verified after sorting at a minimum rate of 80%. Genomic DNA was extracted, and the V3–V4 region of the 16S rRNA gene was amplified by using seminested PCR. The primers V3fwd (+357; 5' TACGGRAGGCAGCAG 3') and V4rev (+857; 5' ATCTTACCAGGGTATCTAATCCT 3') were used during the first round of PCR (10 cycles). The primers V3fwd and X926\_Rev (+926; 5' CCGTCAATTCMTTTRAGT 3') were used in the second PCR round (40 cycles). PCR amplicon libraries were sequenced with a MiSeq Illumina platform (Genotoul, Toulouse, France). The open source software package Quantitative Insights Into Microbial Ecology (QIIME)<sup>13</sup> was used to analyze sequences with the following criteria: (1) minimum and maximum read length of 250 and 500, respectively; (2) no ambiguous base calls; (3) no homopolymeric runs longer than 8 bp; and (4) minimum average Phred score of greater than 27 within a sliding window of 50 bp. Sequences were aligned with NAST against the Greengenes reference core alignment set (available in QIIME as core\_set\_aligned.fasta.imputed) by using the “align\_seqs.py” script in QIIME. Sequences that did not cover this region at a percentage identity of greater than 75% were removed. Operational taxonomic units (OTUs) were picked at a threshold of 97% similarity by using cd-hit from “pick\_otus.py” script in QIIME. Picking workflow in QIIME with the CD-HIT clustering method currently involves collapsing identical reads by using the longest sequence-first list removal algorithm, picking OTUs, and subsequently inflating the identical reads to recapture abundance information about the initial sequences. Singletons were removed because only OTUs that were present at the level of at least 2 reads in more than 1 sample were retained (9413 ± 5253 sequences per sample). The most abundant member of each OTU was selected through the “pick\_rep\_set.py” script as the representative sequence. The resulting OTU representative sequences were assigned to different taxonomic levels (from phylum to genus) by using the Greengenes database (August 2012 release), with consensus annotation from the Ribosomal Database Project naive Bayesian classifier (RDP 10 database, version 6).<sup>14</sup> To confirm the annotation, OTU representative sequences were then searched against the RDP database by using the online program seqmatch ([http://rdp.cme.msu.edu/seqmatch/seqmatch\\_intro.jsp](http://rdp.cme.msu.edu/seqmatch/seqmatch_intro.jsp)) and a threshold setting of 90% to assign a genus to each sequence.

### Immunoblotting

Colony-forming units (10<sup>8</sup>) of wild-type *E coli* were frozen (–80°C) and thawed (37°C) 3 times in 30 µL of lysis buffer (50 mmol/L Tris–HCl and 8 mol/L urea). Lysis efficiency was verified by using gram staining. Proteins were separated by using 4% to 20% polyacrylamide gel electrophoresis (Mini-PROTEAN TGX Stain-Free Precast Gels; Bio-Rad Laboratories) in reducing conditions (dithiothreitol and SDS; Bio-Rad Laboratories) and transferred to nitrocellulose. Membranes were incubated with 10 µg/mL human serum IgG or IgA of different healthy donors. Human IgG was detected with horseradish peroxidase-conjugated goat anti-human IgG used at 1:50,000 or goat anti-human IgG used at 1:20,000, followed by enhanced chemiluminescence revealing reaction (Clarity Western ECL; Bio-Rad Laboratories). Human IgA was detected with horseradish peroxidase-conjugated goat anti-human IgA used at 1:20,000 (Bethyl Laboratories, Montgomery,

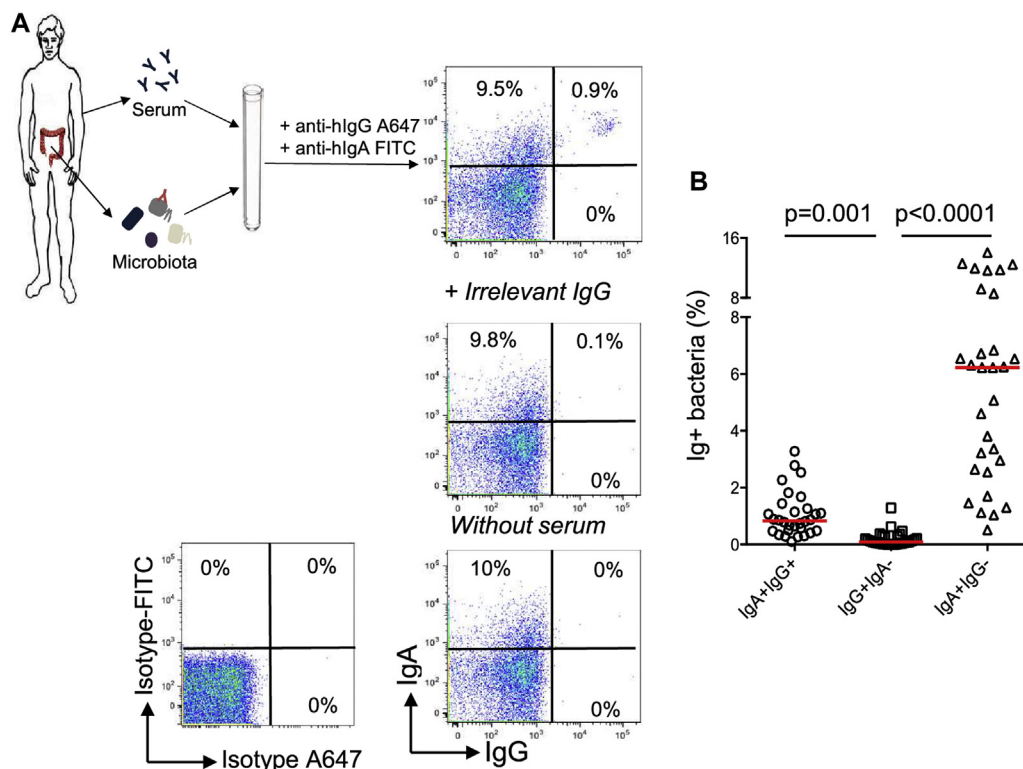


**FIG 1.** Systemic IgG and secretory IgA recognize a common spectrum of commensals. **A**, Representative flow cytometric dot plot showing (from bottom to top) isotype control, endogenous secretory IgA (without serum), human IgG anti-TNF (10  $\mu$ g/mL, irrelevant IgG), and autologous systemic IgG (10  $\mu$ g/mL) to fecal microbiota in a healthy donor. **B**, Flow cytometry analysis of the fraction of fecal microbiota bound by either secretory IgA, serum IgG, or both in healthy donors ( $n = 30$ ). Median values are indicated, and subgroups are compared with a nonparametric Mann-Whitney test.

Tex). All incubations were in  $1 \times$  PBS with 5% nonfat milk and washing steps in  $1 \times$  PBS with 0.1% Tween.

### IgG gene expression analysis

Total RNA of jejunal lamina propria fraction and PBMCs were extracted with the RNeasy Mini kit (Qiagen, Hilden, Germany). cDNAs were synthesized from and prepared with M-MLV reverse transcriptase (Promega, Madison, Wis). SYBR Green primers were designed by the manufacturer (Roche) and used for quantitative RT-PCR with the 7300 real time PCR system (Applied Biosystem, Foster City, Calif). Data were normalized to ribosomal 18S RNA.

## RESULTS

### Convergence of intestinal IgA and serum IgG toward the same bacterial cells

To determine the level of humoral systemic response against fecal microbiota, we have elaborated a flow cytometric assay derived from a previously reported technology.<sup>12</sup> This protocol allows us to probe concomitantly IgA and IgG microbiota coating. We found that approximately 8% of the fecal microbiota is targeted by secretory IgA (median, 8% [minimum-maximum, 0.8% to 26.7%];  $n = 30$ ) in healthy donors in concordance with previous reports.<sup>12</sup> As shown, the proportion of bacteria *in vivo* bound by secretory IgA in human feces is highly variable between healthy subjects (Fig 1, B). IgG-bound bacteria are virtually absent from healthy human feces (median, 0.03% [minimum-

maximum, 0% to 0.16%];  $n = 30$ ; Fig 1, A, and see Fig E1 in this article's Online Repository at [www.jacionline.org](http://www.jacionline.org)), which is in agreement with the lack of IgG transport to the intestinal lumen. In healthy donors serum IgG bound a median rate of 1.1% of fecal bacteria (minimum-maximum, 0.2% to 3.2%; Fig 1, B). Surprisingly, serum IgG targeted exclusively secretory IgA-bound bacteria (Fig 1, A). Conversely, all IgA-coated bacteria (IgA<sup>+</sup> bacteria) were not targeted by serum IgG. Of note, an irrelevant human monoclonal IgG (chimeric anti-human TNF containing a human Fc IgG fraction) exhibits markedly reduced binding to IgA<sup>+</sup> bacteria compared with serum IgG (Fig 1, A, and see Fig E2 in this article's Online Repository at [www.jacionline.org](http://www.jacionline.org)), demonstrating that IgG binding to IgA-coated bacteria is mostly Fab-mediated.

To confirm that systemic IgG binding is directed against IgA-bound bacteria, we evaluated *in vitro* serum IgG binding to culturable bacterial strains. We selected 4 bacterial strains that were not preferentially bound by IgA in human feces and 4 others that were previously defined as classical IgA targets *in vivo*.<sup>15-17</sup> As shown in Fig 2,<sup>18</sup> IgG from healthy subjects ( $n = 30$ ) much more significantly binds *Bifidobacterium longum*, *Bifidobacterium adolescentis*, *Faecalibacterium prausnitzii*, and *Escherichia coli*, which are known to be particularly enriched in the IgA-coated fraction of healthy subjects than 3 different strains of *Bacteroides* species and *Parabacteroides distasonis*, which are known to be particularly enriched in the IgA-uncoated fraction of the fecal microbiota (Fig 2, A and B). The

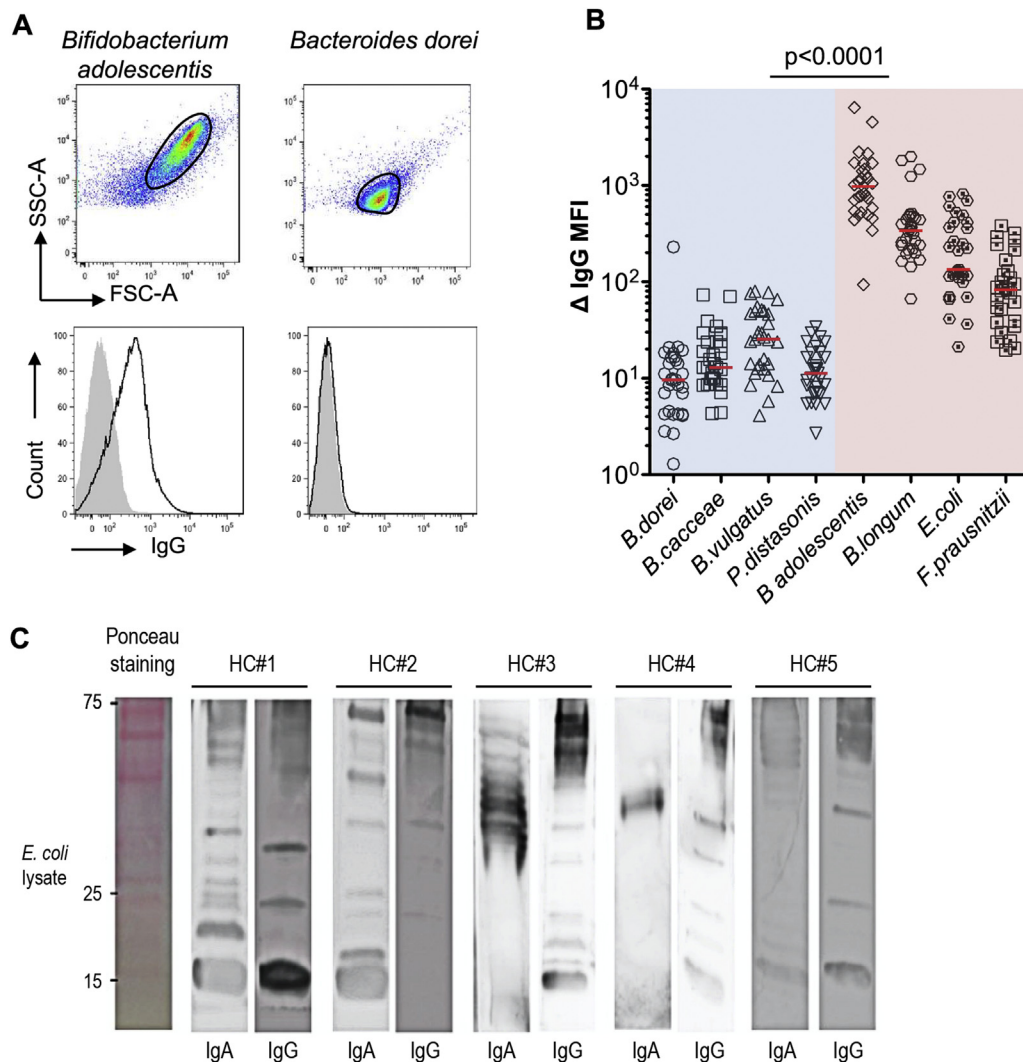


**FIG 2.** Systemic IgG binds a broad spectrum of commensals. **A**, Flow cytometric analysis of serum IgG binding to cultivated bacterial strains. *Gray histograms* represent isotype controls, and *dark lines* represent anti-IgG staining. **B**, Flow cytometric analysis of serum IgG binding levels to 8 different bacterial strains in healthy donors ( $n = 30$ ). Blue strains (*left*) are typically poorly coated by secretory IgA from healthy subjects, and pink strains (*right*) are representative of typical IgA targets.<sup>18</sup> Results are presented as  $\Delta$  median fluorescence intensity (MFI): IgG = MFI IgG serum – MFI IgG negative control. *Red bars* show medians. The Kruskal-Wallis test was used to calculate  $P$  values. **C**, Representative immunoblotting of *E. coli* lysates probed with 5 different healthy human serums, with normalized IgA and IgG levels. Ponceau staining indicates total amounts of bacteria lysates loaded. IgA and IgG binding were assessed by using a horseradish peroxidase-conjugated secondary antibody.

majority of anti-commensal IgG antibodies are of the IgG<sub>2b</sub> and IgG<sub>3</sub> isotypes in mice. Using isotype-specific secondary antibodies, we detected minimal IgG<sub>1</sub> binding but high serum IgG<sub>2</sub> reactivity to *B. adolescentis*, *B. longum*, and *E. coli*, suggesting that IgG<sub>2</sub> is involved in commensals targeting in human subjects (see Fig E3 in this article's Online Repository at [www.jacionline.org](http://www.jacionline.org)).

Because anticommensal IgG can be triggered during mucosal immune responses, we characterized lamina propria B cells and detected the presence of IgG<sub>2</sub><sup>+</sup> B cells throughout the intestine (see Fig E4 in this article's Online Repository at [www.jacionline.org](http://www.jacionline.org)). Of note, IgG transcripts are more abundant in lamina propria tissue than in PBMCs, as measured by using quantitative PCR (see Fig E4).

These results demonstrate that human IgG recognizes a wide range of commensals under homeostatic conditions. Systemic humoral immunity (notably IgG<sub>2</sub>) converges with mucosal immunity to bind the surface of commensals.

#### Interindividual variability and nonoverlapping anticommensal IgA and IgG molecular targets

It was previously suggested that murine IgG would target a restricted number of bacterial proteins and favor highly conserved outer membrane proteins.<sup>8</sup> Reactivity of human serum IgG against bacterial lysates from gram-negative strains was evaluated by means of immunoblotting. We observed that IgG labeled several *E. coli* bands (Fig 2, C), suggesting that multiple bacterial

products are involved in induction of systemic antibodies. Interestingly, this analysis reveals a great deal of interindividual variability because it is not always the same bacterial products that react to the tested sera. We then compared the overlap between bacterial products labeled by IgG and IgA and found distinct binding profiles (Fig 2, C). Finally, in the 5 subjects tested, although some bacterial products (notably a 15-Kda antigen) are frequently targeted in most subjects and without isotype restriction, it clearly appears that IgA and IgG never share exactly the same binding pattern at a molecular level.

Taken together, these results demonstrate that although IgG converges with IgA to bind the surfaces of commensals, it appears that IgA and IgG do not systematically target the same bacterial antigens, even at the individual level.

### Private antimicrobiota IgG specificities are induced in IgA-deficient patients

The existence of serum IgG able to bind IgA-coated bacteria could equally suggest that some gut bacteria (or bacterial antigens) can cross the intestinal barrier either (1) in spite of IgA or (2) because of IgA. To explore these 2 putatively opposing roles for IgA, we studied the systemic anticommensal IgG response in patients with SIgAd. These patients had undetectable serum and digestive IgA levels, whereas serum IgG levels were in the normal range.<sup>18</sup> Antimicrobiota IgG levels were significantly greater in patients with SIgAd compared with those in control subjects (median, 3.3% [minimum-maximum, 0.2% to 20.2%] vs 1.1% [minimum-maximum, 0.2% to 3.2%]; Fig 3, A). Using irrelevant human IgG, we confirmed that, as in healthy donors, IgG interacts with fecal bacteria in a Fab-dependent manner (see Fig E2, B). These data support an enhanced triggering of systemic IgG immunity against fecal microbiota when lacking secretory IgA, as shown in the murine model of polymeric immunoglobulin receptor deficiency.<sup>6</sup>

Considering this high level of antimicrobiota IgG in patients with SIgAd and the similarity of SIgAd and healthy microbiota composition,<sup>18</sup> we investigated how antimicrobiota IgG repertoires from healthy donors and IgA-deficient patients overlapped. Using polyclonal IgG from pooled sera of healthy donors, we assessed IgG-bound microbiota using either healthy or SIgAd-purified microbiota. We showed that pooled polyclonal IgG and autologous healthy sera recognized a similar percentage of fecal bacteria (median, 1% [minimum-maximum, 0% to 3.7%] vs 1.1% [minimum-maximum, 0.2% to 3.2%], respectively; Fig 3, B and C). In contrast, pooled polyclonal IgG bound a smaller bacterial fraction of IgA-deficient microbiota compared with autologous patient serum (median, 0.4% [minimum-maximum, 0% to 3.6%] vs 3.3% [minimum-maximum, 0.2% to 20.2%]; Fig 3, B and C).

To test whether similar specificities are induced in all or most IgA-deficient subjects, we compared their IgG reactivity to autologous or heterologous gut microbiota. In this experiment (Fig 3, D) each IgA-deficient microbiota was incubated either with autologous serum (ie, autologous condition) or with serum from an unrelated IgA-deficient subject (ie, heterologous condition). As shown in Fig 3, D, no significant difference was seen between autologous or heterologous conditions (median autologous IgG<sup>+</sup> microbiota: 1.2% vs median heterologous IgG<sup>+</sup> microbiota: 1.4%). Of note, heterologous serum IgG also predominantly interacts with the fecal microbiota in a Fab-dependent manner (see Fig E2, C).

This set of data suggests that peculiar antimicrobiota IgG specificities are induced in IgA-deficient patients but not in healthy subjects.

### IgG specifically recognizes a broad spectrum of bacteria

To more deeply decipher anticommensal IgG specificities in both healthy donors and IgA-deficient patients, we next performed a stringent flow sorting to isolate IgG-bound bacteria and identified their taxonomy using 16S rRNA sequencing (Fig 4, A). We observed extensive interindividual variability at the genus level, irrespective of immunologic status (healthy donors vs IgA-deficient patients). Microbial diversity calculated by using the Shannon index varied between donors, but on average, bacterial diversity of IgG<sup>+</sup> and IgG<sup>-</sup> bacteria was not significantly different (Fig 4, B). We postulated that IgG might preferentially interact with dominant taxa and therefore compared the relative abundance of IgG-bound and IgG-unbound genera. Both fractions exhibited equal distributions of rare and abundant genera (Fig 4, C), and thus IgG targets commensals irrespective of their frequency. Interestingly, we found that individual IgG<sup>+</sup> and IgG<sup>-</sup> fecal bacterial profiles were remarkably different, supporting a strong IgG bias against peculiar taxa that cannot be explained by an expansion of the latter. In addition, anticommensal IgG was not restricted to pathobionts but also targeted symbiotic genera, such as *Faecalibacterium prausnitzii* having been assigned anti-inflammatory properties in both healthy donors and IgA-deficient patients (Fig 4, D and E).<sup>19</sup> We conclude that anticommensal IgG recognizes a diverse array of both pathobionts and commensal bacteria. Importantly, each subject harbored a private IgG antimicrobial signature.

### High antimicrobiota IgG levels correlate with reduced systemic inflammation

Microbiota-specific serum IgG responses contribute to symbiotic bacterial clearance in the periphery and maintain mutualism in mice.<sup>2</sup> Thus we hypothesized that anticommensal IgG can influence the balance of systemic inflammatory versus regulatory responses in human subjects. Hence we measured plasma levels of sCD14 (a marker of monocyte activation<sup>20</sup>) and observed that serum IgG-coated bacteria inversely correlated with sCD14 ( $r = -0.42$ ,  $P < .005$ ; Fig 5, A) in both healthy donors and patients with SIgAd. These results are in line with the finding that IgG replacement therapy reduced endotoxemia.<sup>21</sup>

To further explore the potential link between antimicrobiota IgG and systemic inflammation, we explored patients with CVID (characterized by both IgG and IgA defects). These patients benefit from intravenous immunoglobulin (IVIg) treatment. Yet we show that IVIg does not efficiently bind CVID microbiota. As shown in Fig 5, B, IVIg bound a reduced fraction of microbiota in patients with CVID compared with control microbiota (median, 0.37% [minimum-maximum, 0.00% to 1.14%] vs 1.06% [minimum-maximum, 0.00% to 3.7%]).

We then determined plasma levels of sCD14 and IL-6 (an inflammatory cytokine reflecting T-cell activation) and evaluated the expression of programmed cell death protein 1 (PD-1; a T-cell coinhibitory molecule induced after activation) on CD4<sup>+</sup> T cells. Both IL-6 and sCD14 levels were consistently greater in patients with CVID than in healthy donors (IL-6: median, 1.8 pg/mL

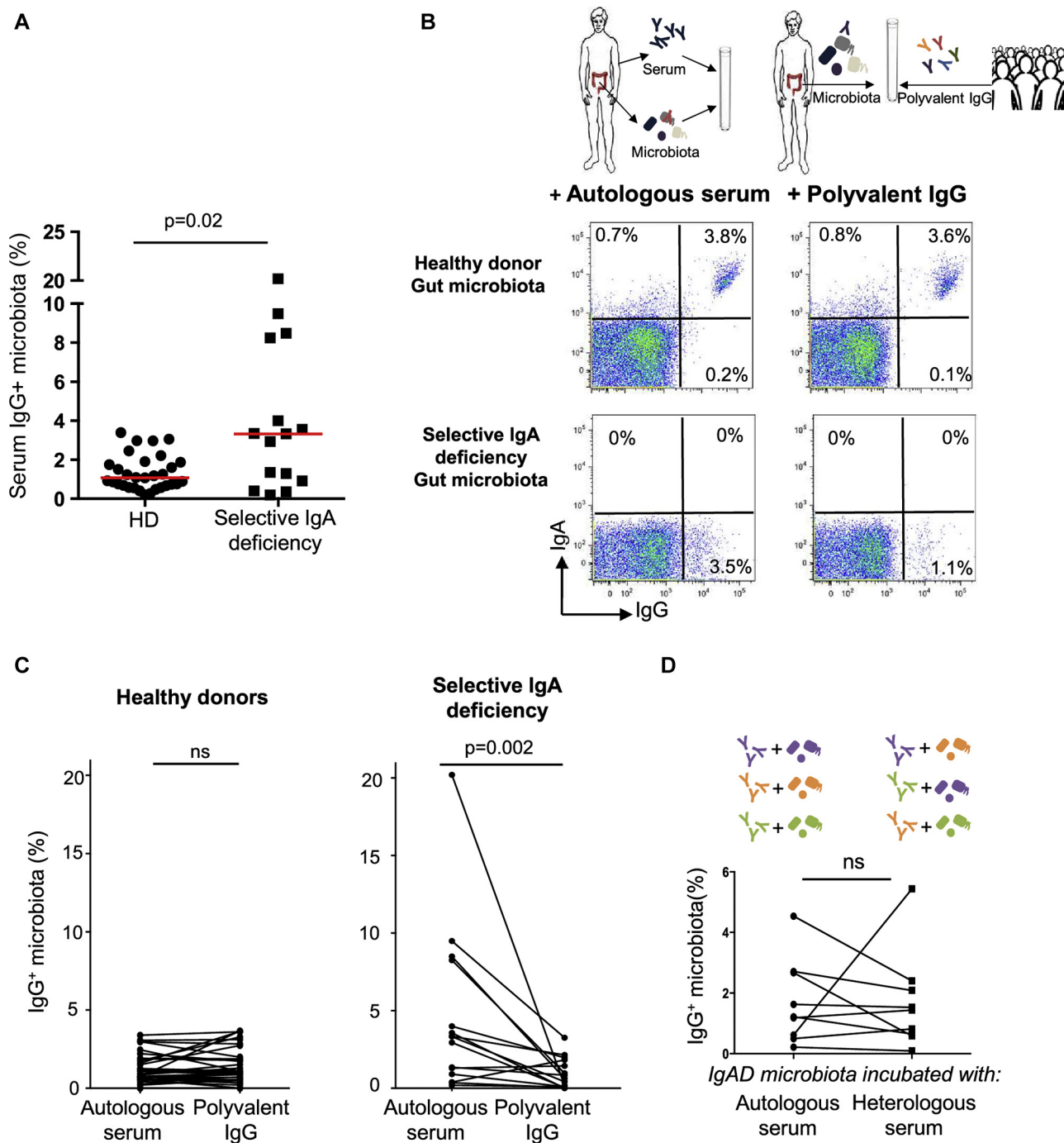


**FIG 3.** IgA-deficient patients harbor private anticommensal IgG responses. **A**, Flow cytometric analysis of fecal microbiota bound by autologous serum IgG in healthy donors ( $n = 30$ ) and IgA-deficient patients ( $n = 15$ ). Red bars represent medians.  $P$  values were calculated by using the Mann-Whitney test. **B**, Representative flow cytometric analysis of autologous serum IgG binding (left) or polyclonal IgG derived from pooled sera of healthy donors binding (right) to fecal microbiota in a healthy donor (top) and an IgA-deficient patient (bottom). **C**, Flow cytometric analysis of the IgG-bound fecal microbiota with IgG from autologous serum or polyvalent IgG in healthy donors ( $n = 30$ ) and IgA-deficient patients ( $n = 15$ ).  $P$  values were calculated by using the Wilcoxon paired test. **D**, Flow cytometric detection of IgG on IgA-deficient microbiota ( $n = 9$ ) after incubation with autologous serum or heterologous serum from another randomly chosen IgA-deficient subject.  $P$  values were calculated by using the Wilcoxon paired test. *ns*, Not significant.

[minimum-maximum, 0.7-60.1 pg/mL] vs 0.6 pg/mL [minimum-maximum, 0.33-2.4 pg/mL]; sCD14: median, 2063 pg/mL [minimum-maximum, 590-5493 pg/mL] versus 2696 pg/mL [minimum-maximum, 1147-4283 pg/mL]; Fig 5, C and D).

Moreover, numbers of  $CD45RA^-PD-1^+CD4^+$  T cells tended to increase in patients with CVID compared with those in healthy donors (median, 20.3% [minimum-maximum, 4.26% to 59.6%] vs 10% [minimum-maximum, 2.09% to 41.9%]; Fig 5, E).

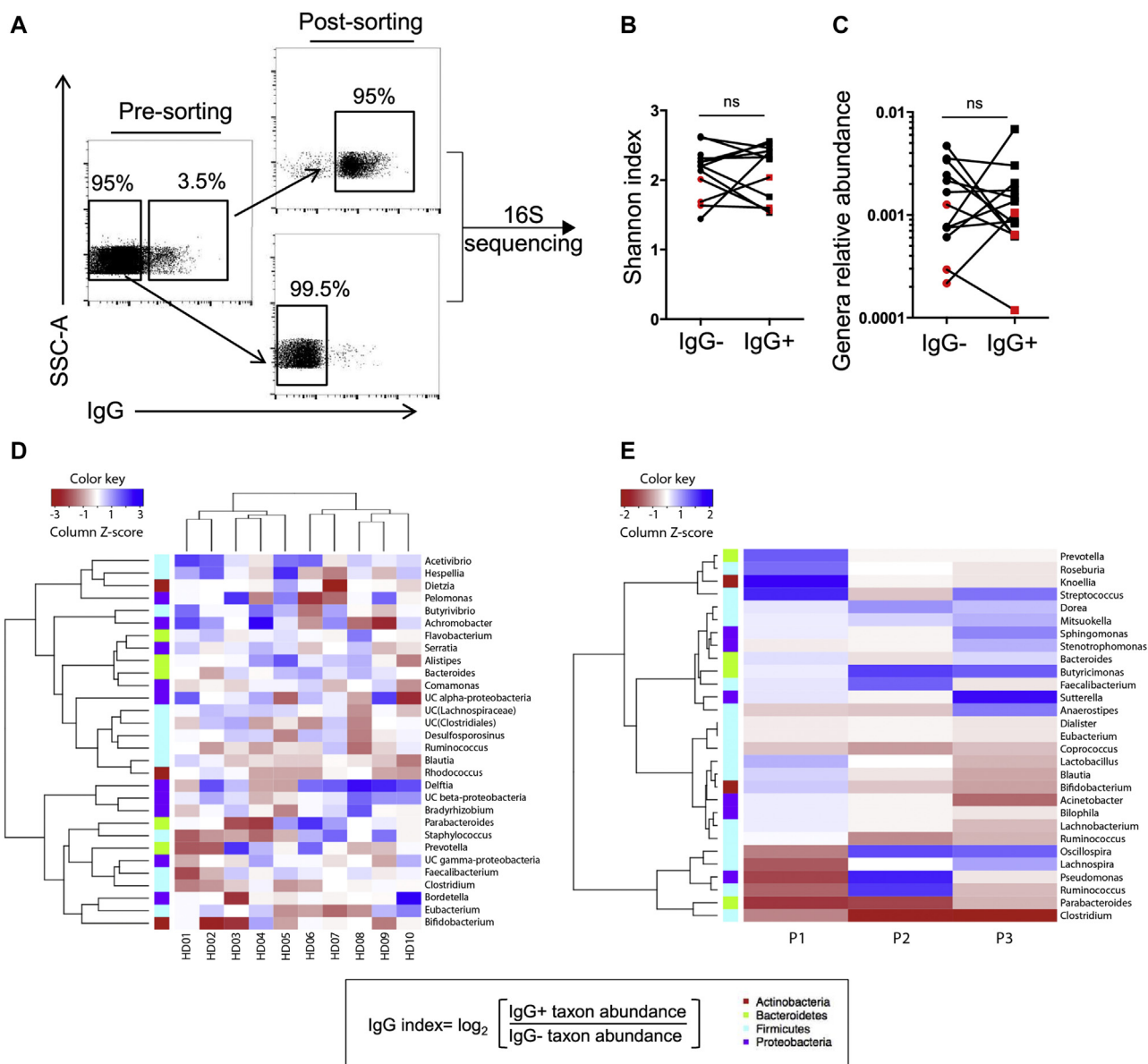


**FIG 4.** Private IgG antimicrobial signatures. **A**, Sorting strategy of IgG-bound and IgG-unbound microbiota in 10 healthy donors and 3 IgA-deficient patients. Composition of sorted subsets was next analyzed by using 16S rRNA sequencing. **B**, Genera diversity in IgG<sup>+</sup> and IgG<sup>-</sup> sorted fractions calculated by using the Shannon index. *Dark symbols* correspond to healthy donors, and *red symbols* correspond to IgA-deficient patients. **C**, Median relative abundance of genera in IgG<sup>+</sup> and IgG<sup>-</sup> sorted fractions. *Dark symbols* correspond to healthy donors, and *red symbols* correspond to IgA-deficient patients. **D**, IgG responses to the 30 most frequent genera in 10 healthy donors. IgG response to a given bacterium is expressed as a calculated IgG index (as defined in the box), outlining genera more likely serum IgG bound in red. Genera and subjects are grouped by using a hierarchical clustering algorithm. **E**, IgG responses (defined by IgG index) to the 30 most frequent genera in 3 IgA-deficient patients. *ns*, Not significant.

Altogether, in both control subjects and IgA-deficient patients, systemic antimicrobiota IgG responses correlate with reduced inflammation.

## DISCUSSION

Anticommensal IgG has been described in patients with inflammatory diseases.<sup>5,22,23</sup> For the first time, we characterize a broad anticommensal IgG response under homeostatic conditions in human subjects. Previous work demonstrated that

symbiotic gram-negative bacteria disseminate spontaneously and drive systemic IgG responses.<sup>8</sup> We show here that a diverse array of commensal bacteria, including gram-positive and gram-negative species, can induce systemic IgG. We show that a pathobiont like *E coli* induces less systemic IgG responses than a presumably beneficial symbiont like *B adolescentis* (Fig 2, B). Therefore the systemic IgG response in healthy human subjects does not appear to be preferentially driven by pathobionts but also by commensals. In mice it has been shown that commensal microbes induce serum IgA responses that protect

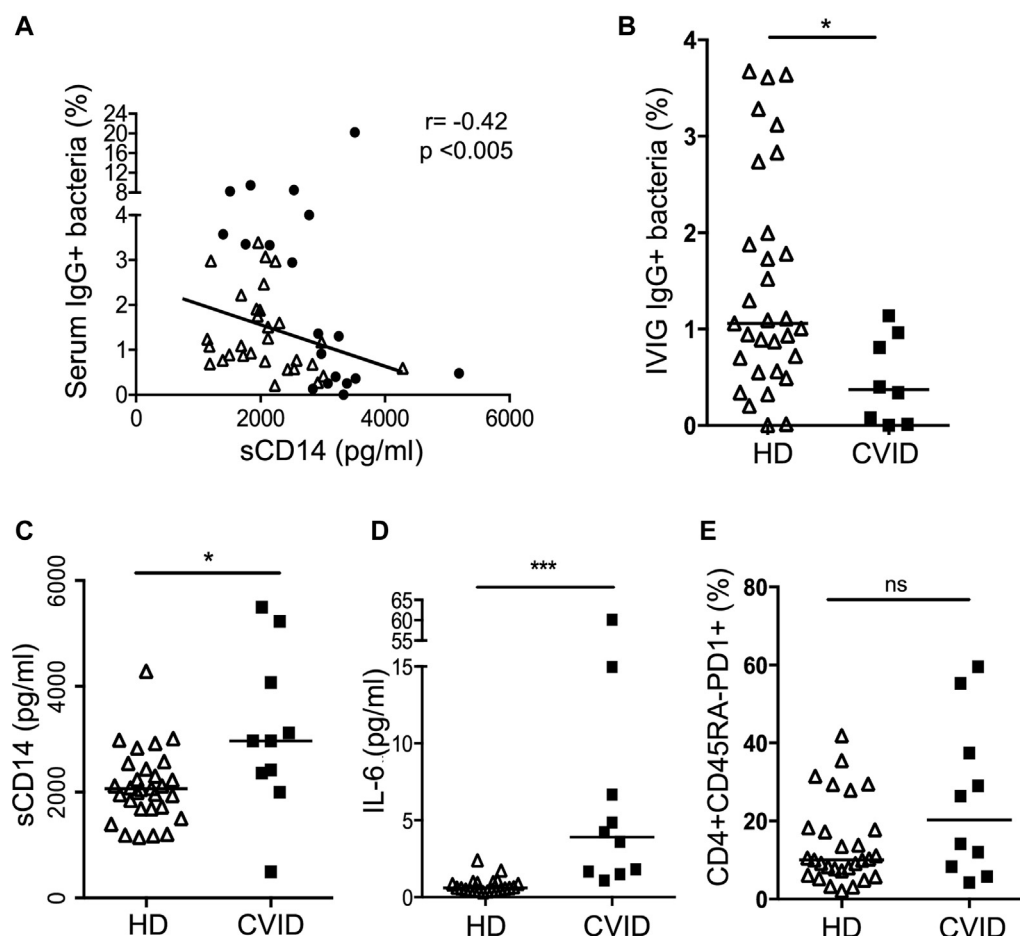


**FIG 5.** Microbiota-specific IgG and inflammation. **A**, Percentage of serum IgG-bound microbiota correlated with sCD14 levels in autologous serum of healthy donors (*triangles*) and patients with SIgAd (*dark points*). Spearman coefficients (*r*) and *P* values are indicated. **B**, Flow cytometric analysis of IgG-bound microbiota after IVIG exposure in healthy donors and patients with CVID. **C**, sCD14 levels measured by means of ELISA in plasma of healthy donors and patients with CVID. **D**, IL-6 levels measured by using Simoa technology in plasma of healthy donors and patients with CVID. **E**, Flow cytometric analysis of CD4<sup>+</sup>CD45RA<sup>+</sup>PD-1<sup>+</sup> lymphocytes in PBMCs of healthy donors and patients with CVID. Percentage among CD4<sup>+</sup> T cells is presented. For all dot plots, *black lines* represent medians. The Mann-Whitney test was used to calculate *P* values as follows: \**P* < .05 and \*\*\**P* < .001. *ns*, Not significant.

against sepsis,<sup>24</sup> illustrating the consequence of systemic antimicrobial IgA binding to both pathogenic strains and commensals. We postulate that systemic antimicrobiota IgG, which is also mainly induced by commensals, could have the same protective role.

Strikingly, systemic IgG and secretory IgA converge toward the same autologous microbiota subset. Yet it seems unlikely that secretory IgA enhances systemic IgG responses because IgA deficiency is associated with high proportions of IgG<sup>+</sup> microbiota, as detected by using bacterial flow cytometry on microbiota of patients with SIgAd labeled with autologous serum. In addition, induction of anticommensal IgG has been shown to be microbiota dependent but IgA independent in mice.<sup>2,6</sup> Systemic IgG could reflect asymptomatic gut microbiota translocation episodes in healthy subjects. Repeated bacterial translocations can occur more frequently in the absence of secretory IgA, accounting for increased antimicrobiota IgG levels in these patients.

IgA does not activate complement through the classical pathway.<sup>25</sup> Interestingly, the anti-*B adolescentis* IgG response

is primarily restricted to the IgG<sub>2</sub> isotype (see Fig E3), which less efficiently triggers the classical route of complement than IgG<sub>1</sub> and IgG<sub>3</sub>.<sup>26</sup> Furthermore, IgG<sub>2</sub> interacts poorly with type I Fcγ receptors, whereas IgG<sub>1</sub> and IgG<sub>3</sub> demonstrate affinity for most Fcγ receptors.<sup>27</sup> These distinct binding patterns have functional consequences. IgG<sub>1</sub> antibodies mediate phagocytosis and induce potent proinflammatory pathways, whereas IgG<sub>2</sub> is involved in dendritic cell or B-cell activation.<sup>28,29</sup> In addition, its specific Fc domain interaction, IgG<sub>2</sub>, is usually but not exclusively associated with anticarbohydrate responses.<sup>30</sup> Recently, IgA was also shown to bind multiple microbial glycans.<sup>31</sup> Thus, IgA and IgG<sub>2</sub> could be viewed as playing similar roles but in different compartments. Recently, much effort has been expended to develop bacterial glycan or protein microarray. Glycomics could represent a new option to better decipher antimicrobiota antibody targets.<sup>30,32</sup>

Importantly, we show that IgA and IgG do not systematically target the same bacterial antigens at an individual level (Fig 2, C). Therefore IgG and IgA epitopes are not strictly overlapping. This

result could further illustrate antibacterial IgA/IgG synergy and explain the absence of isotype competition allowing the observed IgA/IgG costaining of bacteria (Fig 1).

Recent studies suggested that murine secretory IgA is polyreactive and binds a broad but defined subset of microbiota.<sup>33,34</sup> Similarly, up to 25% of intestinal IgG<sup>+</sup> plasmablasts could produce polyreactive antibodies.<sup>9</sup> Therefore we hypothesized that the cross-reactive potential of anticomensal IgG can act as a first line of defense against potentially harmful bacteria. In line with this idea, it can be noted that homeostatic anticomensal IgG confers protection against pathogens, such as *Salmonella* species.<sup>8</sup> Conversely, IgG directed against *Klebsiella pneumoniae*, an opportunistic pathogen, cross-reacts with commensal microbes.<sup>35</sup> Clonally related memory B cells expressing cross-specific anti-*K pneumoniae* antibodies were found in both lamina propria and peripheral blood in human subjects, suggesting that generation of anticomensal antibodies can be triggered in the mucosal compartment. At the same time, anticomensal memory B cells might recirculate in the periphery.<sup>35</sup>

Altogether, it appears possible that bacteria-specific IgG would arise from the gut because all bacteria-specific IgG isotypes we characterized in human sera are also present in the gut (see Fig E4) and also because a large proportion of gut IgG<sup>+</sup> B cells are expected to be commensal specific.<sup>9</sup> However, it remains presently unknown whether serum IgG responses mainly originate from the gut and/or are induced in the periphery after bacterial translocation.

We report that each person harbors a private set of anticomensal IgG in both healthy donors and IgA-deficient patients. Because our analysis was limited to 3 IgA-deficient patients, further study might precisely reveal how SIgAd anticomensal IgG binds a distinct set of commensals. Although IVIG preparations contain an extended set of anticomensal IgG, we observe that IVIG less efficiently binds CVID microbiota. These observations are consistent with reported alterations of gut microbiota in patients with CVID.<sup>36</sup> Microbiota perturbations are also associated with SIgAd. The latter perturbations are less pronounced than in patients with CVID because the presence of IgM appears to preserve SIgAd microbiota diversity.<sup>18</sup> Nevertheless, the IgA deficiency condition is also associated in severe cases with bacterial translocation, colitis, and dysbiosis.

These complications are not accessible to substitutive immunoglobulin replacement therapy.<sup>37</sup> Indeed, IVIG does not appear to contain high enough concentrations and appropriate specificities of anticomensal IgG. As shown in Fig 3, healthy control serum usually less efficiently binds IgA-deficient microbiota than autologous serum. Similarly, IVIG poorly targets CVID gut microbiota (Fig 5, B). In addition, local mucosal antibody responses might be important in regulating microbiota composition in a way that cannot be substituted by IVIG. These findings expand our understanding of why IVIG does not treat gastrointestinal symptoms in patients with CVID and IgA-deficient patients. Dysbiosis and gastrointestinal complications might not be accessible to substitutive immunoglobulin replacement therapy because, as we show, a healthy IgG repertoire does not contain adequate “dysbiotic-specific” antibodies.

Recently, it was shown in mice that maternally derived anticomensal IgG dampens aberrant mucosal immune responses and strengthens the epithelial barrier.<sup>7,38</sup> The contribution of systemic anticomensal IgG to the regulation of microbiota/immune homeostasis was not explored in the latter

studies. Here we show that anticomensal IgG is negatively associated with sCD14, suggesting it might quell inflammation. In support of this, we measured greater levels of sCD14 and IL-6 in plasma of patients lacking both IgA and IgG compared with control values (Fig 5).

Altogether, these data suggest that systemic IgG and intestinal IgA cooperate in different body compartments to limit systemic proinflammatory pathways. Although patients with SIgAd harbor increased levels of serum anticomensal IgG, patients with CVID cannot mount an appropriate IgG response. These findings suggest that microbiota confinement is obtained at the price of a strong inflammatory response in patients with SIgAd, while in CVID patients confinement is lost because immunoglobulin replacement therapy does not substitute for a specific autologous IgG response. Therefore we propose that IgA supplementation might have beneficial effects on gut dysbiosis and systemic inflammatory disorders associated with antibody deficiencies. IgA can be delivered orally through a carrier system, allowing colon delivery. Polymers, such as gellan gum or pectin, are degraded specifically by the colonic microbiota and could thus release polymer-bound IgA locally.<sup>39</sup>

In summary, for the first time, we report a systemic anticomensal IgG response that is restricted to intestinal IgA-coated bacteria in human subjects. We demonstrate that in the absence of IgA, anticomensal IgG responses are amplified and associated with reduced systemic inflammation. Finally, the present study provides new therapeutic perspectives based on IgA supplementation in patients with CVID or SIgAd, whereas SIgAd-derived IgG supplementation can be considered in patients with CVID.

We thank Emma Slack for advice, Jean-Michel Batto for discussions, and Joel Doré, Fabienne Beguet-Crespel, and Emma Slack for providing bacterial strains.

#### Key messages

- Systemic IgG and secretory IgA bind a common spectrum of commensals.
- Increased proportions of IgG<sup>+</sup> microbiota and inflammatory markers in patients with SIgAd.
- IVIG poorly targets gut microbiota in patients with CVID and patients with SIgAd.

#### REFERENCES

1. Honda K, Littman DR. The microbiota in adaptive immune homeostasis and disease. *Nature* 2016;535:75-84.
2. Slack E, Hapfelmeier S, Stecher B, Velykoredko Y, Stiel M, Lawson MA, et al. Innate and adaptive immunity cooperate flexibly to maintain host-microbiota mutualism. *Science* 2009;325:617-20.
3. Donskey CJ. The role of the intestinal tract as a reservoir and source for transmission of nosocomial pathogens. *Clin Infect Dis* 2004;39:219-26.
4. MacFie J. Current status of bacterial translocation as a cause of surgical sepsis. *Br Med Bull* 2004;71:1-11.
5. Beaugerie L, Sokol H. Clinical, serological and genetic predictors of inflammatory bowel disease course. *World J Gastroenterol* 2012;18:3806-13.
6. Johansen FE, Pekna M, Norderhaug IN, Haneberg B, Hietala MA, Krajci P, et al. Absence of epithelial immunoglobulin A transport, with increased mucosal leakiness, in polymeric immunoglobulin receptor/secretory component-deficient mice. *J Exp Med* 1999;190:915-22.
7. Koch MA, Reiner GL, Lugo KA, Kreuk LS, Stanbery AG, Ansaldo E, et al. Maternal IgG and IgA antibodies dampen mucosal T helper cell responses in early life. *Cell* 2016;165:827-41.

8. Zeng MY, Cisalpino D, Varadarajan S, Hellman J, Warren HS, Cascalho M, et al. Gut microbiota-induced immunoglobulin G controls systemic infection by symbiotic bacteria and pathogens. *Immunity* 2016;44:647-58.
9. Benckert J, Schmolka N, Kreschel C, Zoller MJ, Sturm A, Wiedenmann B, et al. The majority of intestinal IgA+ and IgG+ plasmablasts in the human gut are antigen-specific. *J Clin Invest* 2011;121:1946-55.
10. Iversen R, Snir O, Stensland M, Kroll JE, Steinsbo O, Korponay-Szabo IR, et al. Strong clonal relatedness between serum and gut IgA despite different plasma cell origins. *Cell Rep* 2017;20:2357-67.
11. Juste C, Kreil DP, Beauvallet C, Guillot A, Vaca S, Carapito C, et al. Bacterial protein signals are associated with Crohn's disease. *Gut* 2014;63:1566-77.
12. Moor K, Fadlallah J, Toska A, Sterlin D, Balmer ML, Macpherson AJ, et al. Analysis of bacterial-surface-specific antibodies in body fluids using bacterial flow cytometry. *Nat Protoc* 2016;11:1531-53.
13. Caporaso JG, Kuczynski J, Stombaugh J, Bittinger K, Bushman FD, Costello EK, et al. QIIME allows analysis of high-throughput community sequencing data. *Nat Methods* 2010;7:335-6.
14. Cole JR, Wang Q, Cardenas E, Fish J, Chai B, Farris RJ, et al. The Ribosomal Database Project: improved alignments and new tools for rRNA analysis. *Nucleic Acids Res* 2009;37:D141-5.
15. D'Auria G, Peris-Bondia F, Dzungova M, Mira A, Collado MC, Latorre A, et al. Active and secreted IgA-coated bacterial fractions from the human gut reveal an under-represented microbiota core. *Sci Rep* 2013;3:3515.
16. Kau AL, Planer JD, Liu J, Rao S, Yatsunenkov T, Trehan I, et al. Functional characterization of IgA-targeted bacterial taxa from undernourished Malawian children that produce diet-dependent enteropathy. *Sci Transl Med* 2015;7:276ra24.
17. Palm NW, de Zoete MR, Cullen TW, Barry NA, Stefanowski J, Hao L, et al. Immunoglobulin A coating identifies colitogenic bacteria in inflammatory bowel disease. *Cell* 2014;158:1000-10.
18. Fadlallah J, El Kafsi H, Sterlin D, Juste C, Parizot C, Dorgham K, et al. Microbial ecology perturbation in human IgA deficiency. *Sci Transl Med* 2018;10.
19. Sokol H, Pigneur B, Watterlot L, Lakhdari O, Bermudez-Humaran LG, Gratadoux JJ, et al. *Faecalibacterium prausnitzii* is an anti-inflammatory commensal bacterium identified by gut microbiota analysis of Crohn disease patients. *Proc Natl Acad Sci U S A* 2008;105:16731-6.
20. Bazil V, Strominger JL. Shedding as a mechanism of down-modulation of CD14 on stimulated human monocytes. *J Immunol* 1991;147:1567-74.
21. Perreau M, Vigano S, Bellanger F, Pellaton C, Buss G, Comte D, et al. Exhaustion of bacteria-specific CD4 T cells and microbial translocation in common variable immunodeficiency disorders. *J Exp Med* 2014;211:2033-45.
22. Landers CJ, Cohavy O, Misra R, Yang H, Lin YC, Braun J, et al. Selected loss of tolerance evidenced by Crohn's disease-associated immune responses to auto- and microbial antigens. *Gastroenterology* 2002;123:689-99.
23. Macpherson A, Khoo UY, Forgacs I, Philpott-Howard J, Bjarnason I. Mucosal antibodies in inflammatory bowel disease are directed against intestinal bacteria. *Gut* 1996;38:365-75.
24. Wilmore JR, Gaudette BT, Gomez Atria D, Hashemi T, Jones DD, Gardner CA, et al. Commensal microbes induce serum IgA responses that protect against polymicrobial sepsis. *Cell Host Microbe* 2018;23:302-11.e3.
25. Russell MW, Mansa B. Complement-fixing properties of human IgA antibodies. Alternative pathway complement activation by plastic-bound, but not specific antigen-bound, IgA. *Scand J Immunol* 1989;30:175-83.
26. Bindon CI, Hale G, Bruggemann M, Waldmann H. Human monoclonal IgG isotypes differ in complement activating function at the level of C4 as well as C1q. *J Exp Med* 1988;168:127-42.
27. Bruhns P, Iannascoli B, England P, Mancardi DA, Fernandez N, Jorieux S, et al. Specificity and affinity of human Fcγ receptors and their polymorphic variants for human IgG subclasses. *Blood* 2009;113:3716-25.
28. Nimmerjahn F, Gordan S, Lux A. FcγR dependent mechanisms of cytotoxic, agonistic, and neutralizing antibody activities. *Trends Immunol* 2015;36:325-36.
29. White AL, Chan HT, French RR, Willoughby J, Mockridge CI, Roghanian A, et al. Conformation of the human immunoglobulin G2 hinge imparts superagonistic properties to immunostimulatory anticancer antibodies. *Cancer Cell* 2015;27:138-48.
30. Schneider C, Smith DF, Cummings RD, Boligan KF, Hamilton RG, Bochner BS, et al. The human IgG anti-carbohydrate repertoire exhibits a universal architecture and contains specificity for microbial attachment sites. *Sci Transl Med* 2015;7:269ra1.
31. Bunker JJ, Erickson SA, Flynn TM, Henry C, Koval JC, Meisel M, et al. Natural polyreactive IgA antibodies coat the intestinal microbiota. *Science* 2017;358.
32. Christmann BS, Abrahamsson TR, Bernstein CN, Duck LW, Mannon PJ, Berg G, et al. Human seroreactivity to gut microbiota antigens. *J Allergy Clin Immunol* 2015;136:1378-86, e1-5.
33. Bunker JJ, Flynn TM, Koval JC, Shaw DG, Meisel M, McDonald BD, et al. Innate and adaptive humoral responses coat distinct commensal bacteria with immunoglobulin A. *Immunity* 2015;43:541-53.
34. Okai S, Usui F, Yokota S, Hori IY, Hasegawa M, Nakamura T, et al. High-affinity monoclonal IgA regulates gut microbiota and prevents colitis in mice. *Nat Microbiol* 2016;1:16103.
35. Rollenske T, Szijarto V, Lukasiewicz J, Guachalla LM, Stojkovic K, Hartl K, et al. Cross-specificity of protective human antibodies against *Klebsiella pneumoniae* LPS O-antigen. *Nat Immunol* 2018;19:617-24.
36. Jorgensen SF, Trosheid M, Kummén M, Anmarkrud JA, Michelsen AE, Osnes LT, et al. Altered gut microbiota profile in common variable immunodeficiency associates with levels of lipopolysaccharide and markers of systemic immune activation. *Mucosal Immunol* 2016;9:1455-65.
37. Favre O, Leimgruber A, Nicole A, Spertini F. Intravenous immunoglobulin replacement prevents severe and lower respiratory tract infections, but not upper respiratory tract and non-respiratory infections in common variable immune deficiency. *Allergy* 2005;60:385-90.
38. Gomez de Agüero M, Ganal-Vonarburg SC, Fuhrer T, Rupp S, Uchimura Y, Li H, et al. The maternal microbiota drives early postnatal innate immune development. *Science* 2016;351:1296-302.
39. Sandolo C, Pechine S, Le Monnier A, Hoys S, Janoir C, Coviello T, et al. Encapsulation of Cwp84 into pectin beads for oral vaccination against *Clostridium difficile*. *Eur J Pharm Biopharm* 2011;79:566-73.

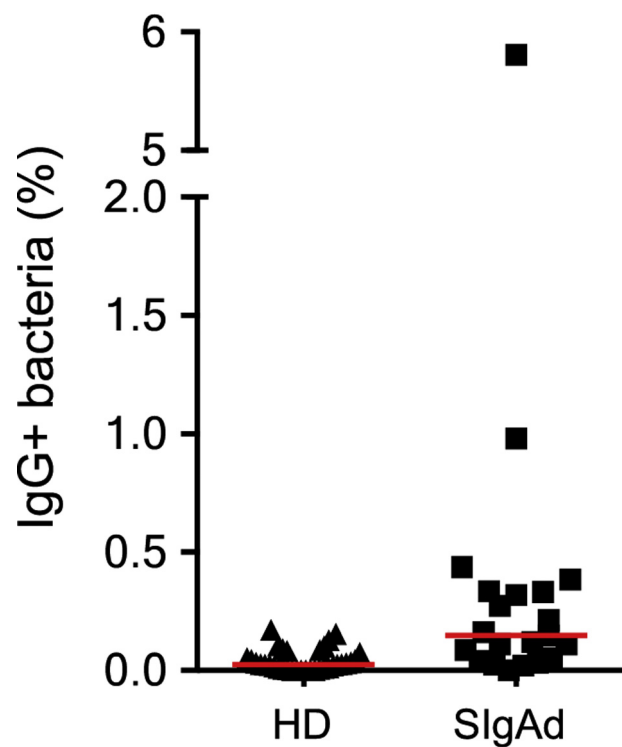


**FIG E1.** *In vivo* intestinal IgG binding to gut microbiota. Flow cytometric analysis of the fraction of fecal microbiota bound by intestinal IgG in healthy donors (HD; n = 30) and patients with SIgAd (n = 15). Pink bars represent medians.

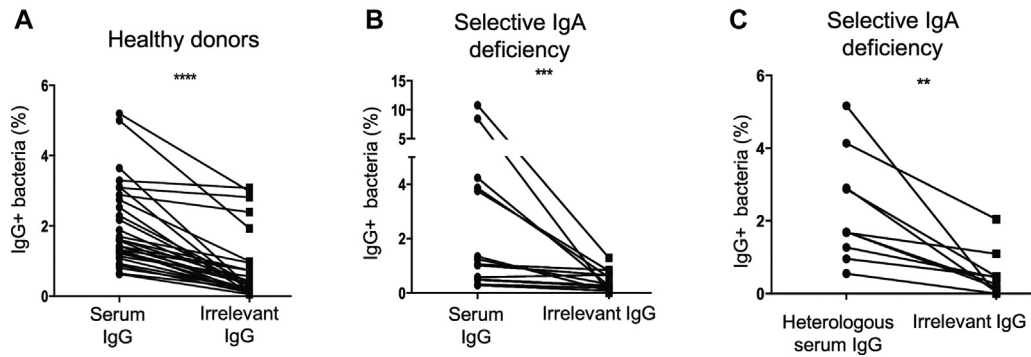


**FIG E2.** Anticommensal IgG reacts mostly in a Fab-dependent manner. **A** and **B**, Flow cytometric analysis of 30 healthy (Fig E2, **A**) and 15 IgA-deficient (Fig E2, **B**) fecal microbiota samples incubated with serum IgG or human IgG anti-TNF. **C**, Flow cytometric analysis of 10 IgA-deficient fecal microbiota samples incubated with heterologous serum IgG or human IgG anti-TNF. The Wilcoxon paired test was used to calculate *P* values as follows: \*\**P* < .01, \*\*\**P* < .001, and \*\*\*\**P* < .0001.

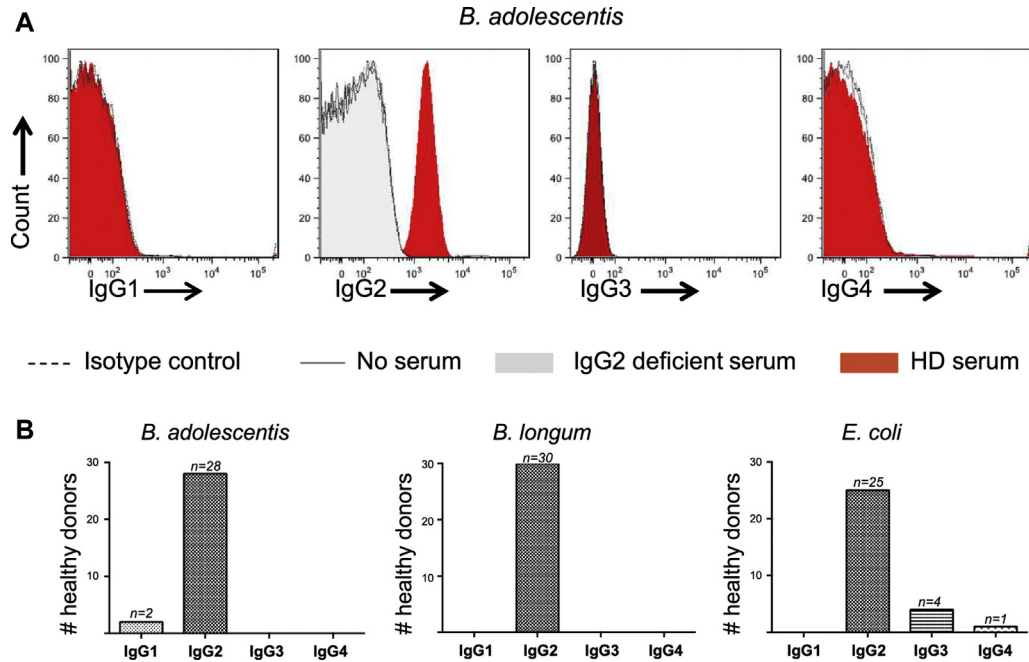


**FIG E3.** Anticommensal IgG is mostly of the IgG<sub>2</sub> isotype. **A**, Representative flow cytometric analysis of serum IgG<sub>1</sub>, IgG<sub>2</sub>, IgG<sub>3</sub>, and IgG<sub>4</sub> binding to *Bifidobacterium adolescentis*. Gray histograms represent serum from an IgG<sub>2</sub>-deficient patient who served as a negative control, and red histograms represent serum from a healthy donor. This donor was scored IgG<sub>2</sub><sup>+</sup> and IgG<sub>1</sub><sup>-</sup> against *B. adolescentis*. **B**, Flow cytometric analysis of IgG<sub>1</sub>, IgG<sub>2</sub>, IgG<sub>3</sub>, and IgG<sub>4</sub> binding to *B. adolescentis*, *Bifidobacterium longum*, and *Escherichia coli* in 30 healthy donors.

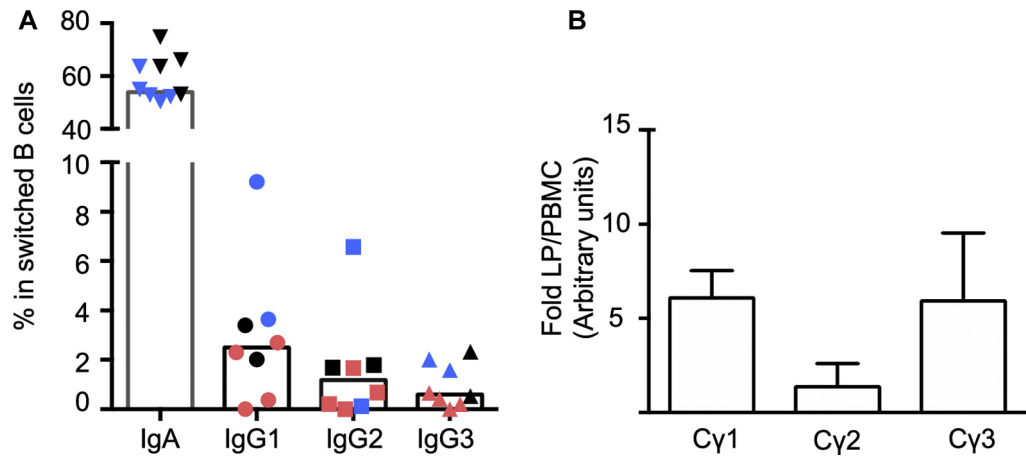


**FIG E4.** IgG<sub>2</sub><sup>+</sup> B cells are present in human gut lamina propria. **A**, Proportions of surface IgA<sup>+</sup>, IgG<sub>1</sub><sup>+</sup>, IgG<sub>2</sub><sup>+</sup>, or IgG<sub>3</sub><sup>+</sup> cells among lamina propria CD19<sup>+</sup>CD27<sup>+</sup>IgD<sup>-</sup> switched B cells were detected by using flow cytometry in jejunum (n = 4, pink symbols), ileum (n = 2, black symbols), or colon (n = 2, blue symbols) samples. **B**, C<sub>γ</sub> transcripts were determined by using quantitative RT-PCR in lamina propria (LP) and PBMCs from 4 severely obese patients. Results are expressed as fold expression in LP over PBMCs (mean ± SEM).